



Strong Magnetic Field driven Spin Density Waves in Pressured Black Phosphorus

Liang-Jian Zou

Institute Solid State Physics
Chinese Academy of Sciences

Singapore 2017/9/21

Contents



- **1. Motivation:**
exp. & theor. Interests on pressured black phosphorus
- **2. Evolutions of Electronic Structures with P**
S-SM transition, 3D Dirac semimetal, Lifshitz transit...
- **3. Density wave of BP in Strong Magnetic Field**
SDW transition, chirality...
- **4. Summary**

1. Research Motivations: experimental aspects

A New 2D Material: Black phosphorus

ARTICLES

PUBLISHED ONLINE: 2 MARCH 2014 | DOI: 10.1038/NNANO.2014.35

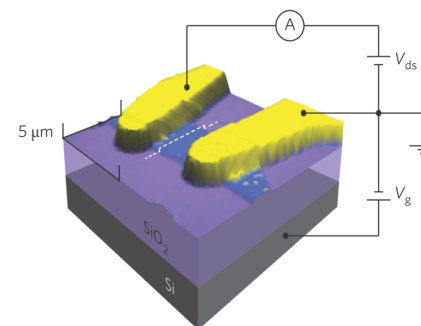
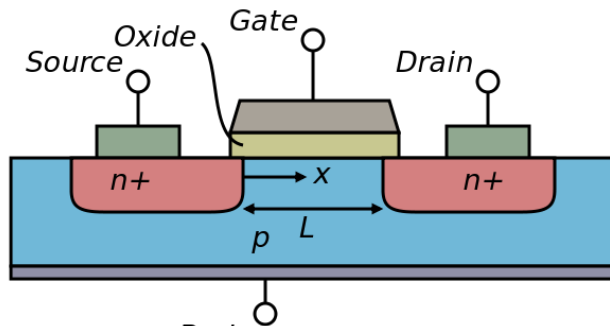
nature
nanotechnology

Black phosphorus field-effect transistors

Likai Li¹, Yijun Yu¹, Guo Jun Ye², Qingqin Ge¹, Xuedong Ou¹, Hua Wu¹, Donglai Feng¹, Xian Hui Chen^{2*} and Yuanbo Zhang^{1*}

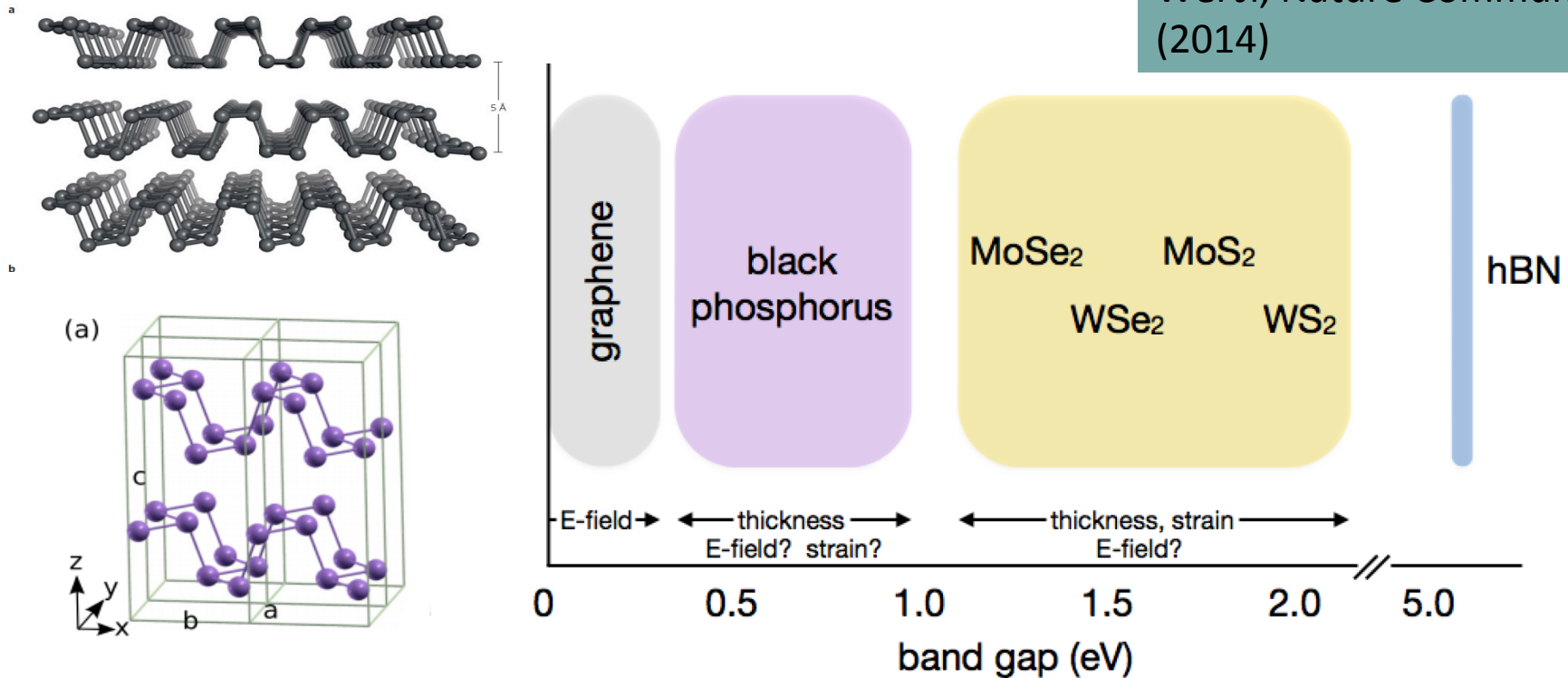
6 ¹² C Carbon 12.011 1s ² 2s ² 2p ² 11.2603	7 ¹⁴ N Nitrogen 14.007 1s ² 2s ² 2p ³ 14.5341
14 ²⁸ Si Silicon 28.086 [Ne]3s ² 3p ² 8.1517	15 ³⁰ P Phosphorus 30.973762 [Ne]3s ² 3p ³ 10.4867
32 ⁷² Ge Germanium 72.63 [Ar]3d ¹⁰ 4s ² 4p ² 7.8994	33 ⁷⁴ As Arsenic 74.92160 [Ar]3d ¹⁰ 4s ² 4p ³ 9.7886

Two-dimensional crystals have emerged as a class of materials that may impact future electronic technologies. Experimentally identifying and characterizing new functional two-dimensional materials is challenging, but also potentially rewarding. Here, we fabricate field-effect transistors based on few-layer black phosphorus crystals with thickness down to a few nanometres. Reliable transistor performance is achieved at room temperature in samples thinner than 7.5 nm, with drain current modulation on the order of 10^5 and well-developed current saturation in the I - V characteristics. The charge-carrier mobility is found to be thickness-dependent, with the highest values up to $\sim 1,000 \text{ cm}^2 \text{ V}^{-1} \text{ s}^{-1}$ obtained for a thickness of $\sim 10 \text{ nm}$. Our results demonstrate the potential of black phosphorus thin crystals as a new two-dimensional material for applications in nanoelectronic devices.



BP: direct band gap optical & electronic properties

Wei Ji, Nature Commun.
(2014)



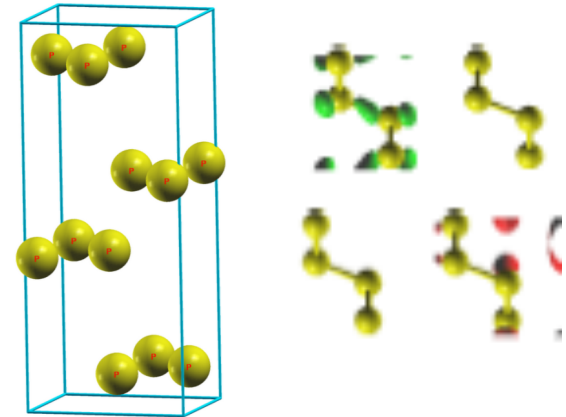
Superior electrical properties: high mobility ($\sim 1000\text{cm}^2/\text{Vs}$), very large turn-off ratio (~ 10000), comparable to traditional Si

Topological origin of 3D Dirac Semimetal ?

Topology of Crystal Structure: nonsymmorphic symmetry

Under ambient & pressure, space group of BP, $Cmca$,

Symmetry operation elements: glide planes

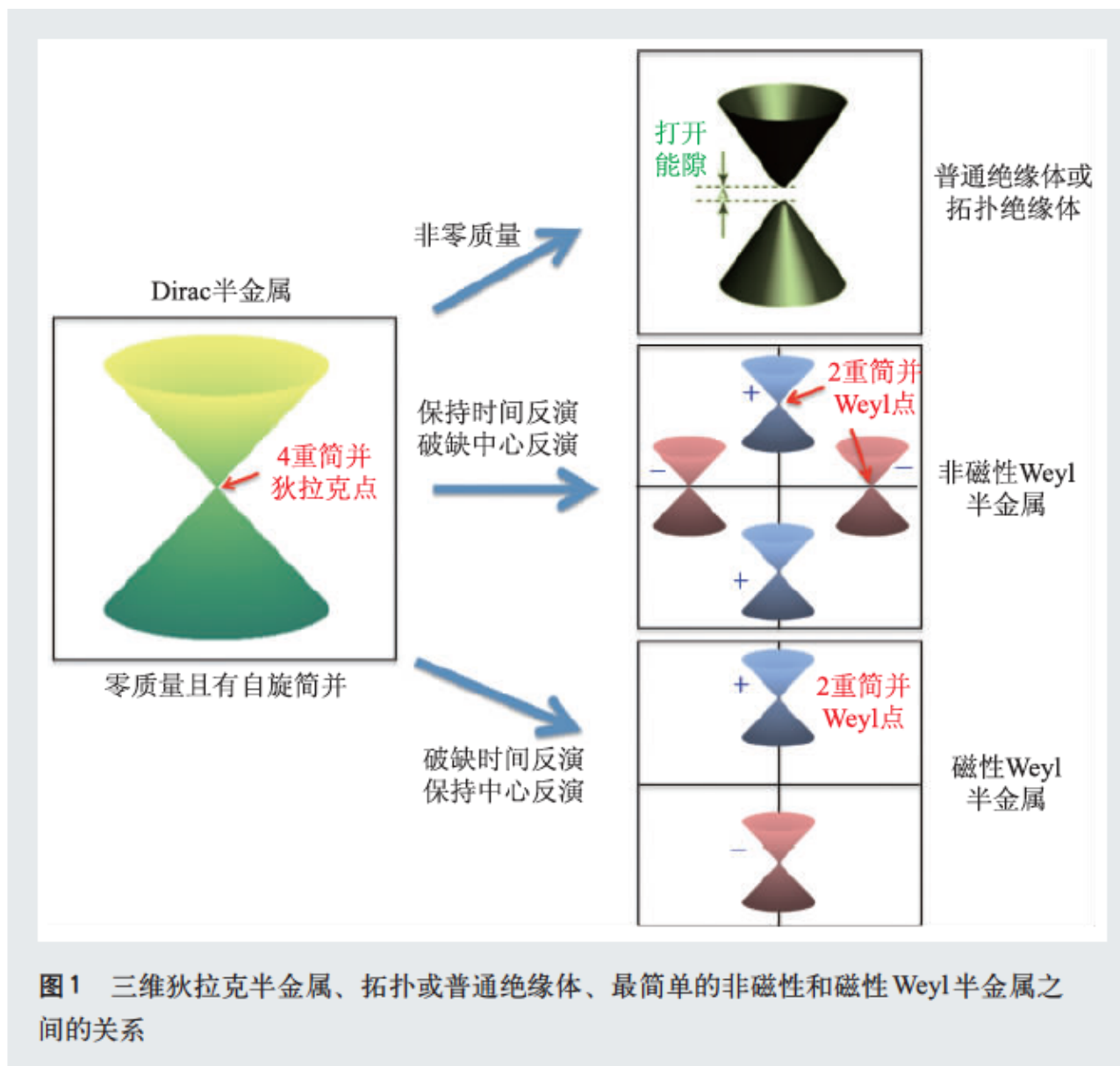


Gibson & Cava, et al. 2015, Phys. RevB. 91. 205128

CASE III: 3D DIRAC SEMIMETALS FROM GLIDE PLANES AND SCREW AXES

The effects of "non-symmorphic" symmetry, or space groups containing glide planes and/or screw axes, on the electronic band structure of solids has been known for a long time [45]. The essence is that the presence of these symmetry elements makes it such that the normally two-fold degenerate bands must touch at four fold degenerate points at certain special points at the surface of the Brillouin zone, and that some of these degeneracies are not

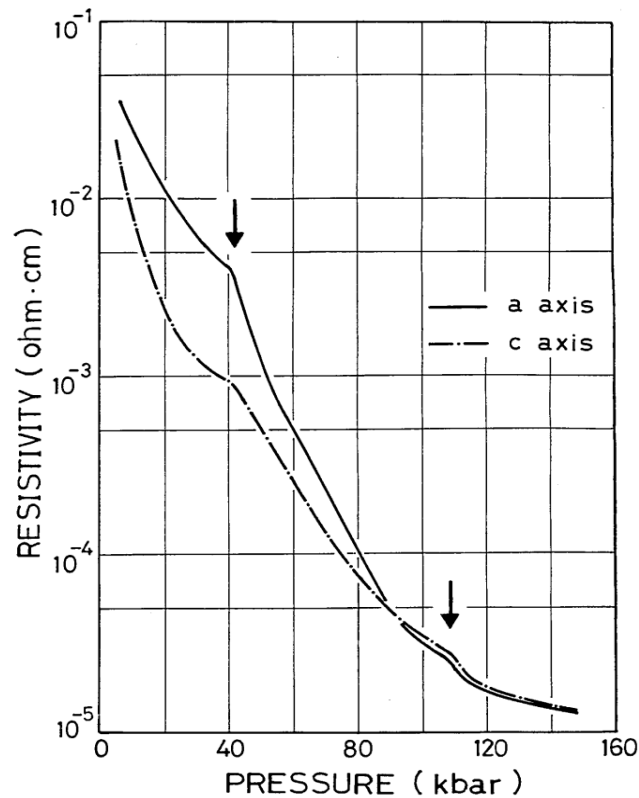
Why 3D Dirac Semimetals interested ?



Weng, Fang, Dai
 <<Physics>>,
 2015

BP in hydrostatic pressure: Phase diagram & S-M transition

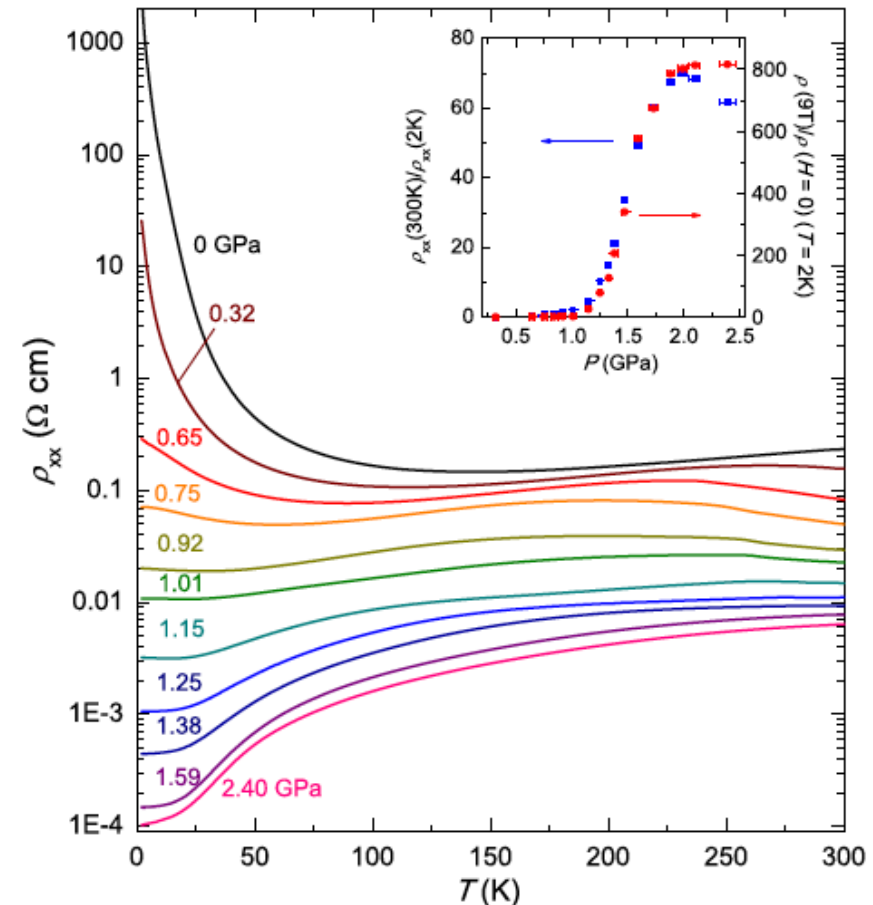
Phase Diagram



4.2 GPa: orthorhombic --> rhombohedral
 10.8 GPa: rhombohedral --> simple cubic

JAPANESE JOURNAL OF APPLIED PHYSICS
 VOL. 23, NO. 1, JANUARY, 1984 pp. 15-19

Resistivity - T



Semicond.-metal transition $P_c \sim 1$ GPa
 X.-H. Chen group, PRL 115, 186403 (2015)

Research Motivations:

What happen in BP: pressure + magnetic field

- Nontrivial topological properties of 3D Dirac semimetal?
- (a). Band inversion, Dirac points & linear energy spectrum ?
- (b). 3D form of 2D graphene: gapless topological semimetals
- (c). In the critical point of various topological materials
- (d). Fermi arc on surface, large g factor, linear MR,

- 3D Dirac Semimetals, derived through modifying field/parameters:
- (e). Topological Insulators
- (f). Weyl semimetals
- (i). Topological SC: gapless zero energy mode : Majorana fermions
- (j).....

2. Electronic structures under pressure

Methods: VASP, Quantum Espresso, WIEN2K,

Exchange-correlation potential:

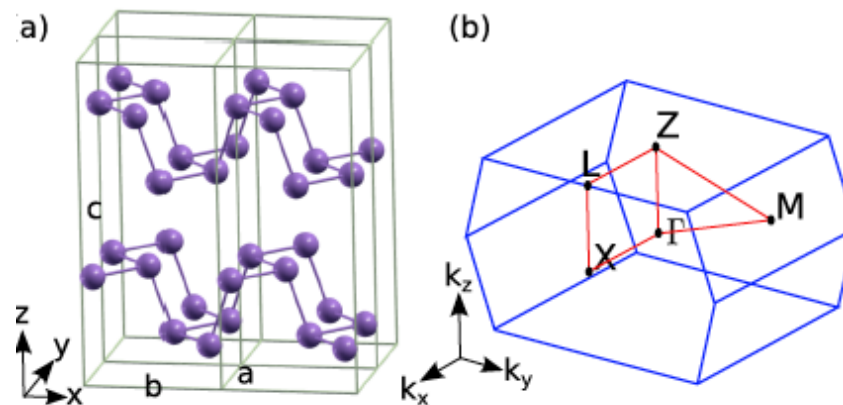
- PBE

Band gap corrections

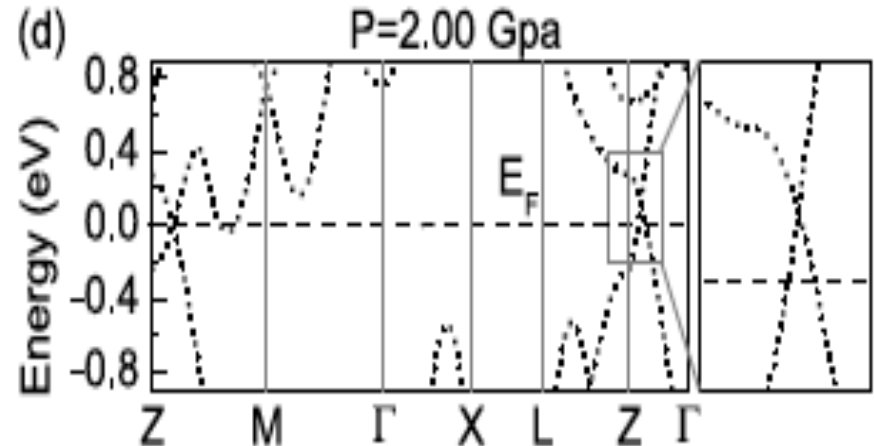
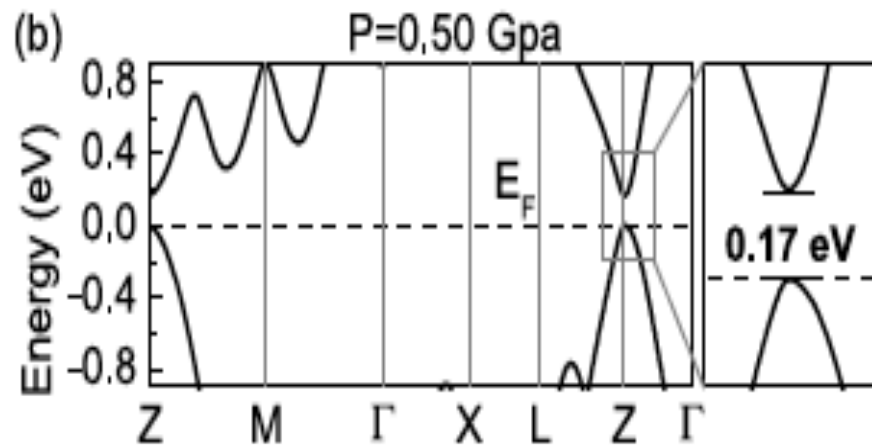
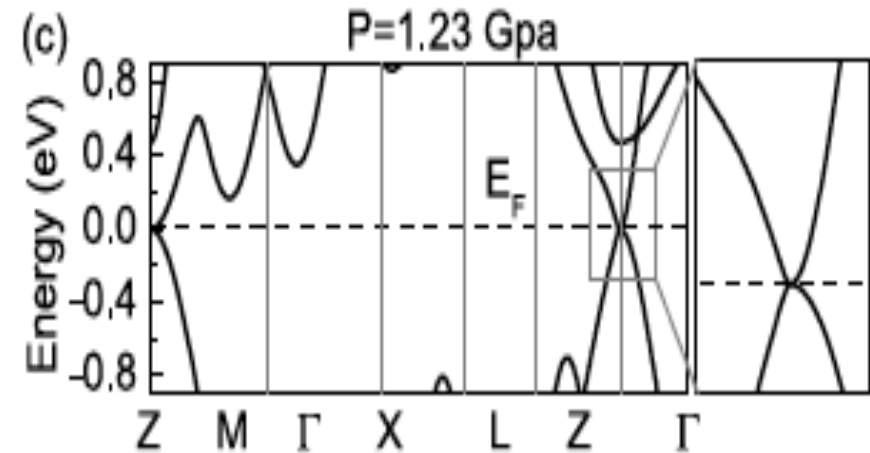
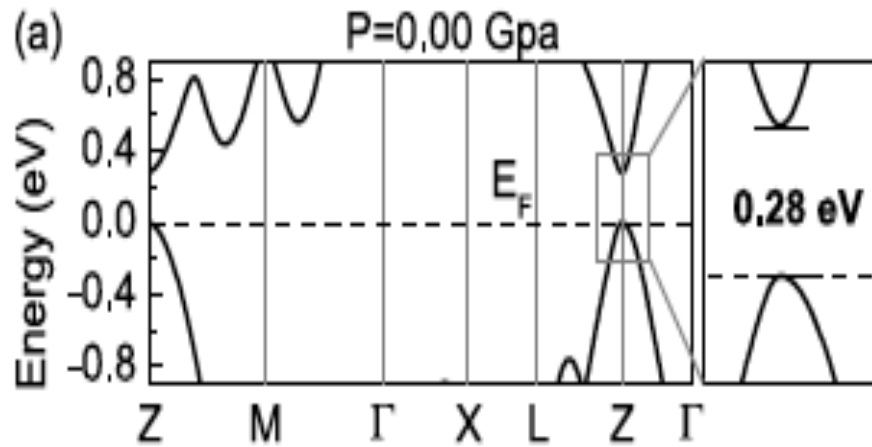
- mBJ
- HSE

Structure optimization

- Vdw: opt-vdw



Evolutions of Band structures with pressure



S-M transition: $P_c=1.23$ eV

DOS & Dirac Cones: 3D Dirac Semimetal

P=1.23 GPa: 3D Dirac Semimetal

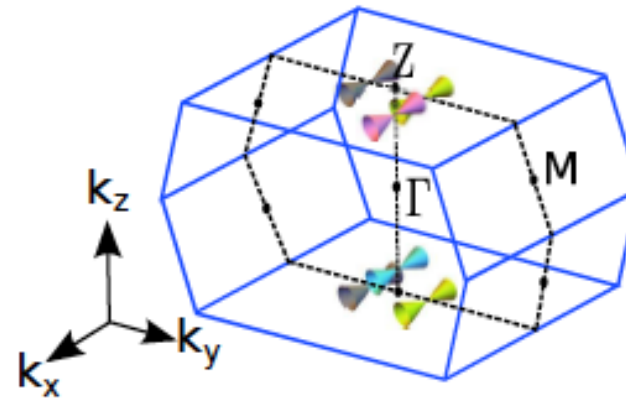
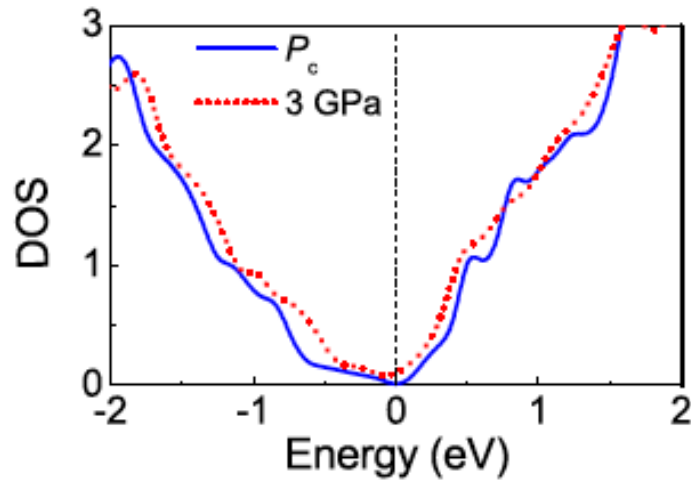
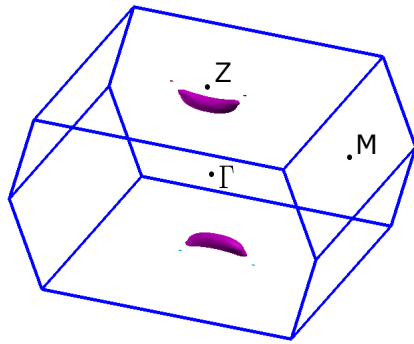


TABLE II. Effective masses of black phosphorus under various hydrostatic pressures and comparison with Refs. [11,37].

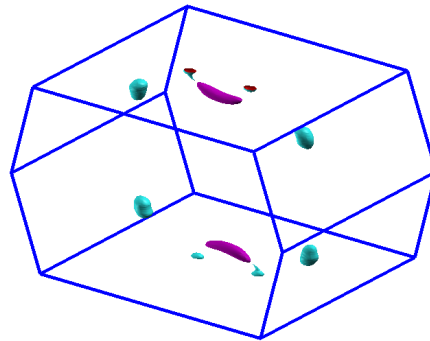
	P(GPa)	m_x^*/m_0	m_y^*/m_0	m_z^*/m_0
e	0.00	0.14(0.12 [11], 0.08 [37])	1.26(1.15 [11], 1.03 [37])	0.16(0.15 [11], 0.13 [37])
	0.50	0.09	1.24	0.14
	1.00	0.05	1.21	0.13
h	0.00	0.12(0.11 [11], 0.07 [37])	0.90 (0.71 [11], 0.65 [37])	0.34 (0.30 [11], 0.28 [37])
	0.50	0.08	0.82	0.32
	1.00	0.04	0.78	0.31

Fermi surface evolution with pressure: Lifshitz transition

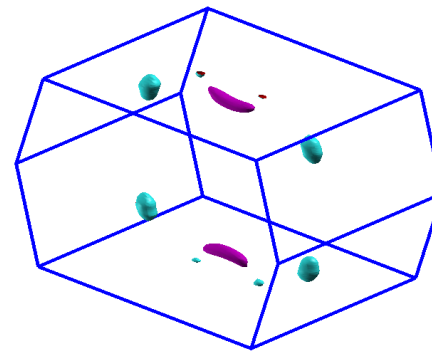
P=1.5 GPa



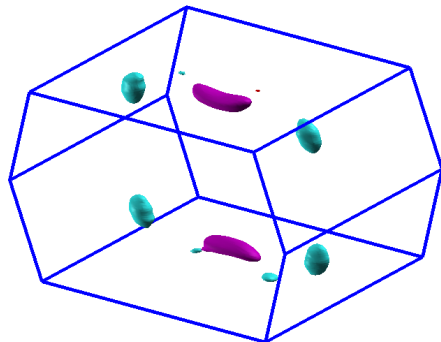
P=2.0 GPa



P=3.0 GPa

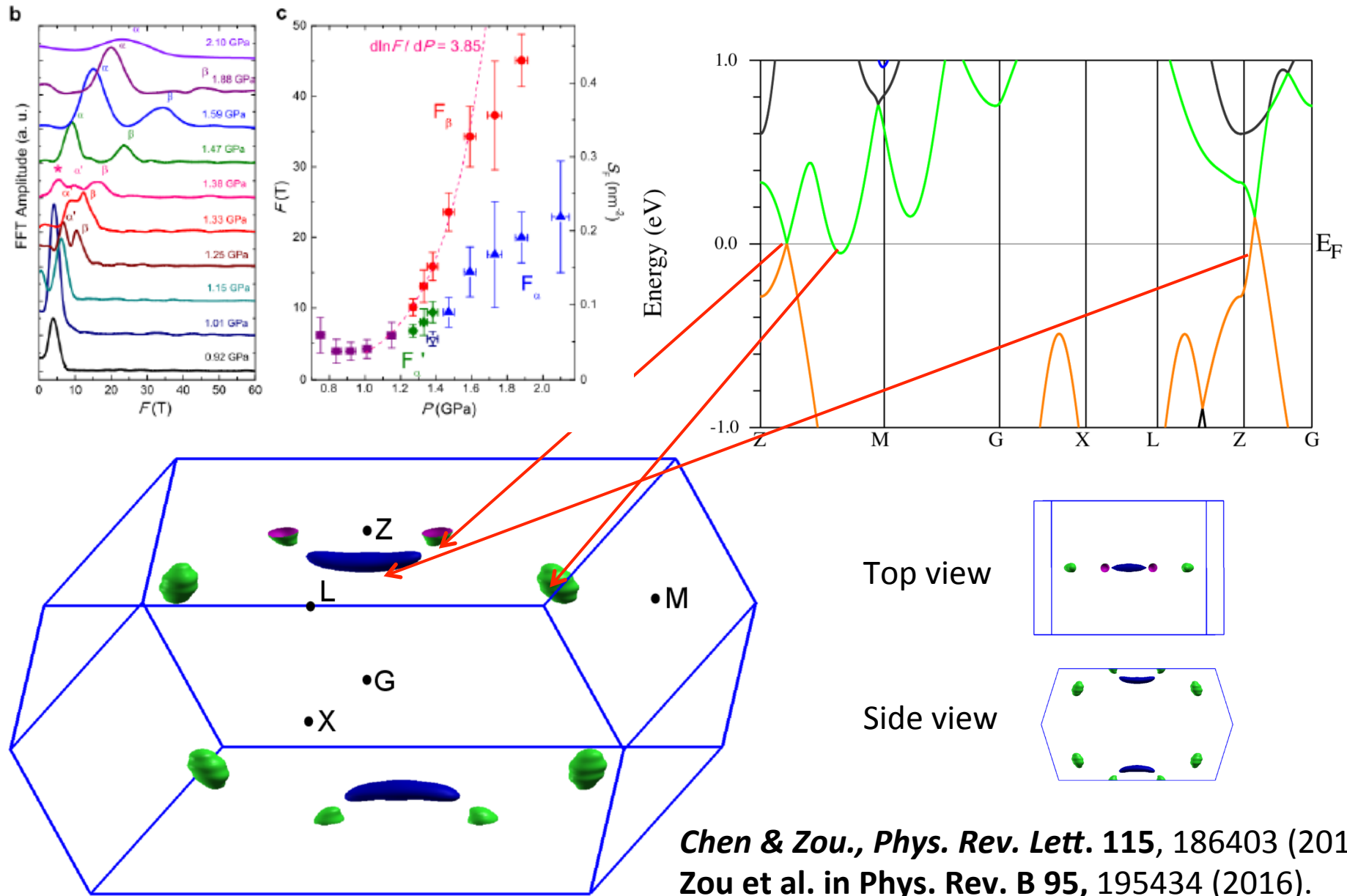


P=4.0 GPa



Pockets type	β (hole)	α (electron)	α^* (electron)
	1.06 ^a	0.4 ^a	0.23 ^a
S_F (nm ⁻²)	(0.42) ^b	(0.22) ^b	(0.16) ^c
Inequivalent numbers	2	4	2
Total S_F (nm ⁻²)	2.12	1.60	0.46

Fermi surfaces & Band structures

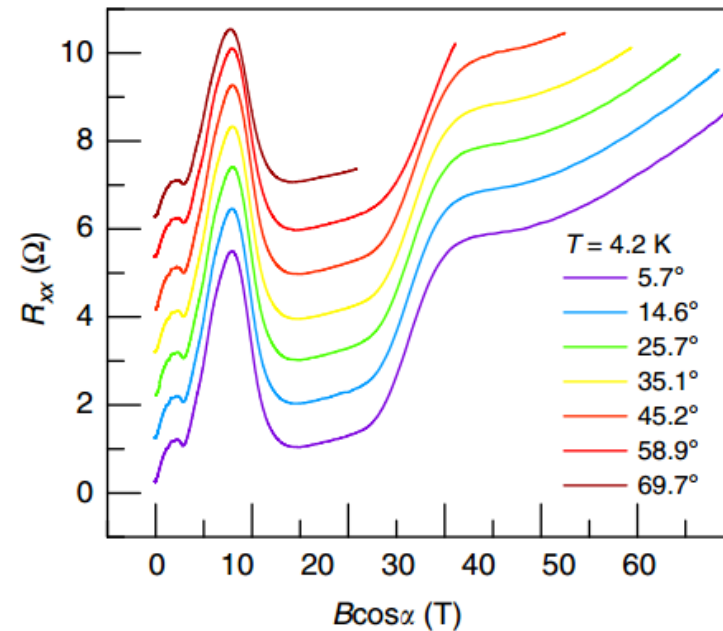
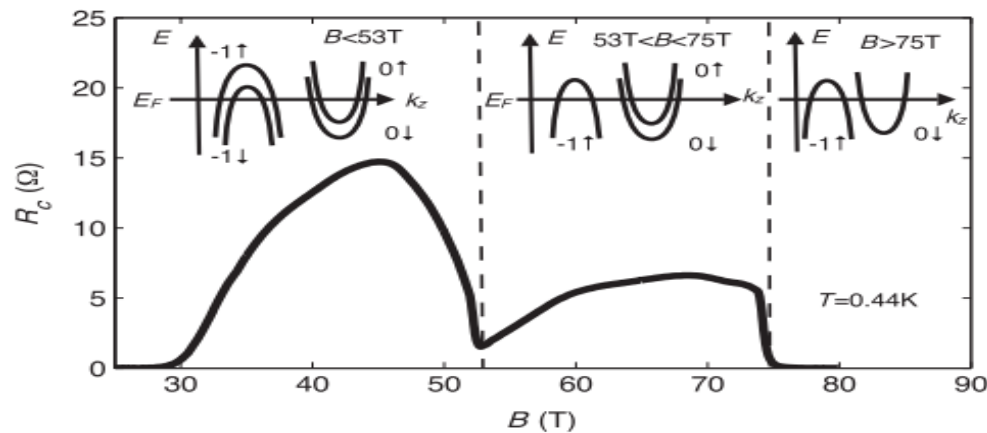


Chen & Zou., Phys. Rev. Lett. 115, 186403 (2015)
Zou et al. in Phys. Rev. B 95, 195434 (2016).

3. 3D Dirac Semimetal in Pressured BP: Strong Magnetic Field Effect

Layered Graphite Semimetal

ZrTe5: 3D Dirac Semimetal



Anomalous increase in R_{xx} :
Why? Exciton condensation
Charge density wave
Spin density wave
... still hotly debated

Model Hamiltonian of 3D Dirac Semimetal BP

Similar to ZrTe5, bulk BP has symmetry of D_{2h} point group below P<4.5 Gpa:

At P around Pc for 3D Dirac semimetal, we have linear Dirac spectrum

$$m_{xz} : \Psi(k_x, k_y, k_z) \rightarrow -\tau^z \cdot i\sigma^y \cdot \Psi(k_x, -k_y, k_z),$$

$$m_{yz} : \Psi(k_x, k_y, k_z) \rightarrow i\sigma^x \cdot \Psi(-k_x, k_y, k_z),$$

$$H_0(k) = \hbar(v_x k_x \tau_x \sigma_z + v_y k_y \tau_y + v_z k_z \tau_x \sigma_x)$$

$$I : \Psi(k_x, k_y, k_z) \rightarrow \tau^z \cdot \Psi(-k_x, -k_y, -k_z),$$

$$\mathcal{T} : \Psi(k_x, k_y, k_z) \rightarrow \mathcal{K} \cdot i\sigma^y \cdot \Psi(-k_x, -k_y, -k_z).$$

Landau Gauge: Landau level quantization in xy plane; free motion in z-axis

$$H = \sum_{k, \sigma} (\sqrt{v_z^2 \hbar^2 k^2 + 2\hbar v_x v_y eBn}) a_{k, \sigma}^+ a_{k, \sigma} + \frac{U}{N} \sum_{k, k', q, \sigma} a_{k, \sigma}^+ a_{k+q, \sigma} a_{k', -\sigma}^+ a_{k'-q, -\sigma}$$

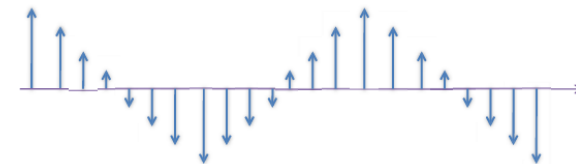
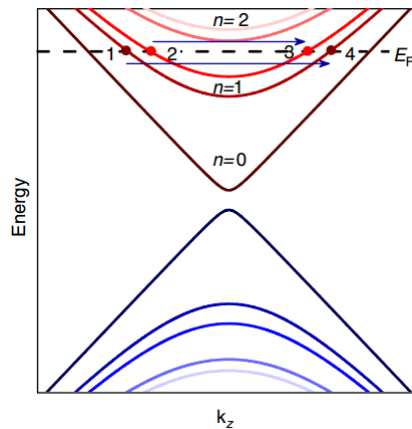
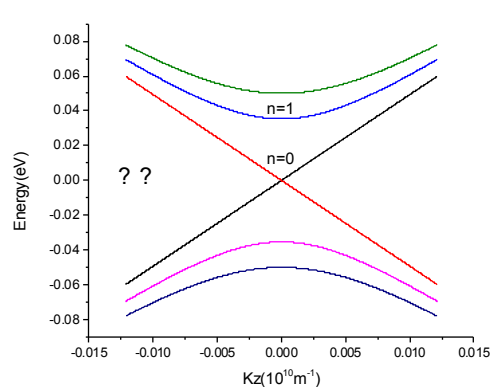


Figure 15. The spin density from the $n = 0$ Landau level.

Focus on the quantum limit: Landau level index $n=0$

(a) on-site Coulomb Interaction:

$$H = \sum_{k,\sigma} v_z \hbar |k| a_{k,\sigma}^+ a_{k,\sigma} + \frac{U}{N} \sum_{k,k',q,\sigma} a_{k,\sigma}^+ a_{k+q,\sigma} a_{k',-\sigma}^+ a_{k'-q,-\sigma}$$

SDW order parameter:
$$\Delta s(q = 2k_F) = \frac{U}{N} \sum_{k,\sigma} \sigma a_{k,\sigma}^+ a_{k+q,\sigma}$$

Chiral SDW order parameter:
$$\Delta s(q = 2k_F) = \frac{U}{N} \sum_k a_{k,\sigma}^+ a_{k+q,-\sigma}$$

$n=0$ SDW energy gap (a,b,c lattice constant)

$$|\Delta|_0 = 2E_F \exp\left(-\frac{(2\pi\hbar)^2 v_z}{eBUabc}\right) = 2E_F \exp\left(-\frac{B^*}{B}\right)$$

One gets critical magnetic field B^* is about $10^4 \sim 10^5$ T, so the on-site repulsive Hubbard model is not applicable !

(b) Long-range Screened Coulomb Interaction:

$$V_c = \frac{1}{2} \int d^3\vec{r}_1 d^3\vec{r}_2 V_c(\vec{r}_1 - \vec{r}_2) \rho(\vec{r}_1) \rho(\vec{r}_2) \quad V_c(\vec{r}_1 - \vec{r}_2) = \frac{e^2 \exp(-k_s |\vec{r}_1 - \vec{r}_2|)}{4\pi\epsilon |\vec{r}_1 - \vec{r}_2|}$$

To replace the on-site U

Self-consistent equation for energy gap of SDW:

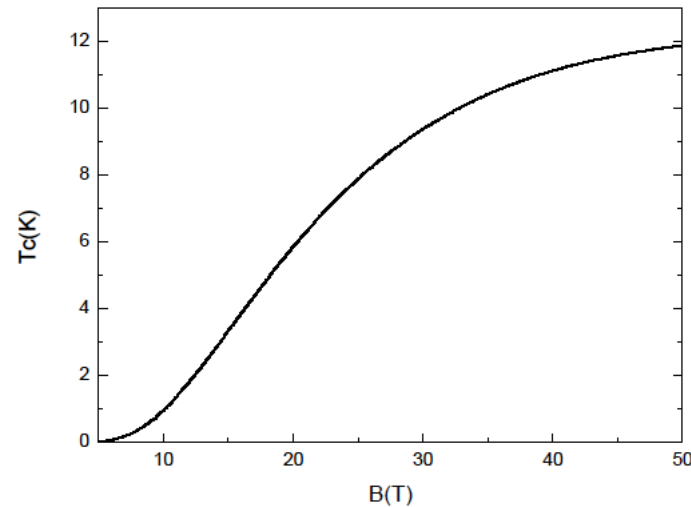
$$\frac{4\varepsilon_0\varepsilon_r\Delta_{k_{x,z}}}{e^2} = \frac{1}{(2\pi)^2} \int_{-\frac{\pi}{a}}^{\frac{\pi}{a}} dk'_x \int_{-k_F}^{k_F} dk'_z \frac{\Delta_{k'_{x,z}}}{2\sqrt{|\Delta_{k'_{x,z}}|^2 + (\hbar v_F k'_z)^2}} \frac{\exp\left\{\frac{l_B^2[(k_z - k'_z)^2 + k_s^2]}{2}\right\}}{\sqrt{(k_x - k'_x)^2 + (k_z - k'_z)^2 + k_s^2}}$$

$$\times \text{Erfc}\left(\frac{l_B \sqrt{(k_x - k'_x)^2 + (k_z - k'_z)^2 + k_s^2}}{\sqrt{2}}\right) \times \tanh\left(\frac{\sqrt{|\Delta_{k'_{x,z}}|^2 + (\hbar v_F k'_z)^2}}{2k_B T}\right)$$

$$\frac{4\varepsilon\Delta_{k_{x,z}}}{e^2} = \int \frac{dk'_x dk'_z}{(2\pi)^2} \frac{\Delta_{k'_{x,z}}}{2\sqrt{|\Delta_{k'_{x,z}}|^2 + (\hbar v_z k'_z)^2}} \frac{\exp\left\{\frac{l_B^2[(k_z - k'_z)^2 + k_s^2]}{2}\right\}}{\sqrt{\delta k^2 + k_s^2}} \text{Erfc}\left(\frac{l_B \sqrt{\delta k^2 + k_s^2}}{\sqrt{2}}\right)$$

here the screening constant k_s is comparable with Fermi wavevector $k_s = 0.2 \times 10^9 \text{ m}^{-1}$, the relative dielectric constant =4, carrier $n = 2.4 \times 10^{23} \text{ m}^{-3}$ is taken from the experimental observation.

Why not CDW ? weak e-ph coupling in BP



SDW of 3D Dirac semimetals

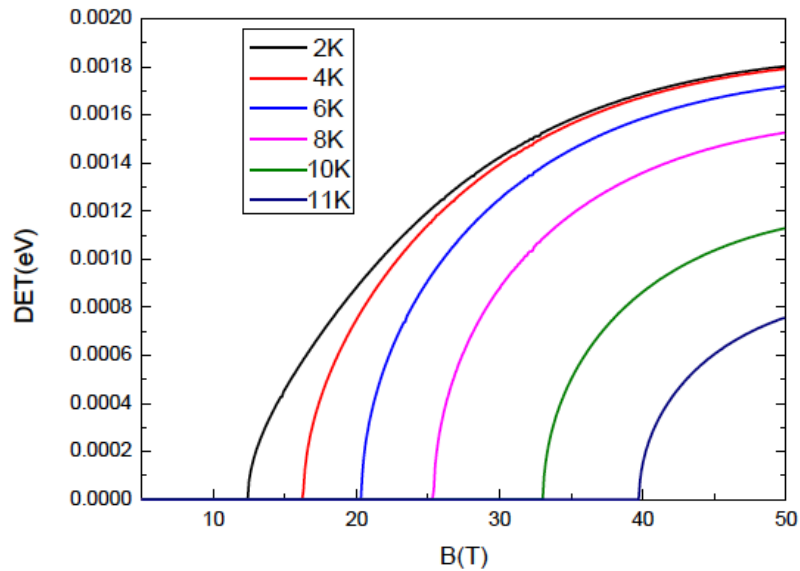


Fig.1a. Depend. of energy gap on applied field

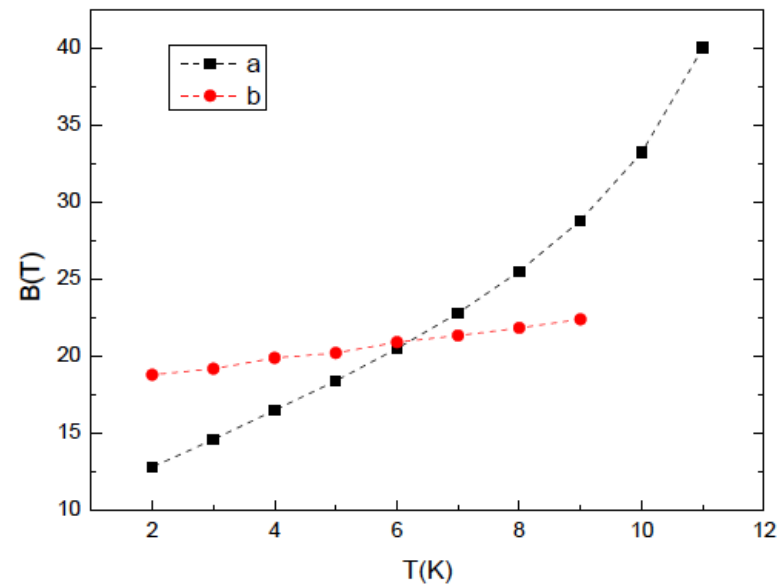


Fig.1b Depend. of critical field B_c on T
Black: theory. Red: recent exp.

Why SDW chiral ? Dirac particles are chiral, particular spins form density wave

we expect more exciting properties in the future.

4. Summary

Hydrostatic pressure effects: confirmed

- At $P=0$, gap ~ 0.27 eV (mBJ) or 0.34 (HSE)
- $P_c = 1.23$ GPa: semicond.-metal transition \rightarrow Lifshitz transition
- $P \sim 1.5$ GPa: Dirac points appear near Z point
- $P > 2.5$ GPa: 2 Fermi pockets (hole & electron) + a Dirac point

Strong Magnetic Field Effects: predicted

- A 3D Dirac semimetal-SDW transition
 - SDW critical magnetic field $B_c \approx 15$ T at $T=2$ K
 - Critical field B_c approx. linearly increases with T
-
- Expect more rich quantum phases in 3D Dirac semimetals



Thanks for your attention !